Copy 274
RM E52A25

NACA

RESEARCH MEMORANDUM

COLD-AIR INVESTIGATION OF A TURBINE WITH NONTWISTED ROTOR BLADES SUITABLE FOR AIR COOLING

By Thomas R. Heaton, William R. Slivka
and Leonard F. Westra

Lewis Flight Propulsion Laboratory
Cleveland, Ohio

NATIONAL ADVISORY COMMITTEE
FOR AERONAUTICS

WASHINGTON
March 18, 1952

NATIONAL ADVISORY COMMITTEE FOR AERONAUTICS

RESEARCH MEMORANDUM

COLD-AIR INVESTIGATION OF A TURBINE WITH NONTWISTED ROTOR BLADES SUITABLE FOR AIR COOLING

By Thomas R. Heaton, William R. Slivka
and Leonard F. Westra

SUMMARY

The performance characteristics of a turbine with nontwisted rotor blades suitable for air cooling were determined. The turbine-design requirements were the same as those of the turbine of a contemporary turbojet engine; geometric departures from the design of the existing turbine were made only where simplicity of cooling the rotor blades would result. The performance characteristics were determined by obtaining the over-all performance and flow surveys of a scale model of this turbine in a cold-air turbine rig.

A brake internal efficiency of 0.82 was obtained at the design equivalent shaft work and design equivalent tip speed. Brake internal efficiencies of the order of 0.845 occurred at stagnation-pressure ratios and equivalent tip speeds greater than design. Large regions of stagnation-pressure loss were present at the stator exit, which indicated possible flow separation on the suction surface of the stator blades. A decrease of turbine efficiency toward the tip of the blade was observed from the flow surveys at the rotor exit.

INTRODUCTION

The application of internal turbine-rotor-blade cooling to aircraft-gas turbines introduces new problems in turbine aerodynamic research. These problems must be considered in the successful and rapid development of cooled turbines. One of the problems is to determine the satisfactory aerodynamic design and the performance of a turbine having rotor blades that are structurally suitable for air cooling. Such a blade could be one of uniform camber and zero twist along the radius with thick trailing edges. This design would be a departure from conventional turbine designs that have twisted rotor blades with thin trailing edges. A nontwisted rotor blade would facilitate the fabrication of rotor blades where internal cooling passages within the blades are desired. Obtaining a cooled-rotor-blade design with satisfactory cooling characteristics near the trailing edge is difficult because of the complexity of providing for cooling passages in a blade with thin trailing edges.

An analytical investigation of the aerodynamic characteristics of nontwisted rotor blades in combination with twisted stator blades is described in reference 1. A study of the performance of turbine blades with thick trailing edges is presented in reference 2. The results of the investigation reported in reference 1 indicate that the aerodynamic-design parameters of nontwisted-rotor-blade turbines generally approximate those of free-vortex turbines intended for similar applications. The results of reference 2 indicate that for a blade with a thin trailing edge having a fixed initial loss, the increase in blade loss due to a thick trailing edge is a function of the ratio of the trailing-edge thickness to the pitch. The results of reference 2 also indicate that for normal two-dimensional blade losses (between 3 and 5 percent) a deterioration in turbine efficiency could be expected if trailing-edge thickness to pitch ratios greater than 0.026 are used.

The results of an experimental investigation of a nontwisted-rotor-blade turbine run successively in combination with (a) twisted stator blades designed to maintain zero rotor entrance incidence angles at all radii, and (b) nontwisted stator blades designed to maintain zero rotor-entrance incidence at the mean radius only are presented in reference 3. The rotor blades of this turbine had a thin trailing edge which was not readily adaptable to air cooling. At approximately the design point, a brake internal efficiency of 0.86 was obtained with this turbine for case (a), which was approximately 1.5 percentage points higher than the brake internal efficiency obtained for case (b).

In order to evaluate the aerodynamic characteristics of turbines with nontwisted rotor blades having thick trailing edges that are suitable for air cooling, a turbine was designed and an experimental investigation of a 0.437 scale model of this turbine was made at the NACA Lewis laboratory. The design requirements of this turbine were the same as those of the turbine of a contemporary turbojet engine; this turbine was designed to maintain zero rotor-entrance incidence angles at all radii. The investigation was conducted in a single-stage turbine rig having a tip diameter of 15 inches with entrance conditions of atmospheric pressure and a temperature of 685° R. Over-all performance data of the turbine were obtained over a range of equivalent tip speeds from 350 to 700 feet per second and stagnation-pressure ratios from 1.5 to 3.0. Circumferential and radial survey data of the flow at the stator and rotor exits were also obtained at approximately design stagnation-pressure ratio and equivalent tip speed.

TURBINE DESIGN

General Specifications

The turbine-design conditions specified were such that the turbine would be required to drive the compressor of a contemporary turbojet engine. When the geometric dimensions of the jet-engine turbine together with the compressor-performance data are used, the following design specifications of the turbine result for sea-level static conditions. The symbols used are defined in appendix A.

Turbine-entrance temperature, T_1', $^\circ R$	2065
Turbine-entrance pressure, p_1', lb/sq ft absolute	10,253
Tip speed, U_t, ft/sec	1185
Equivalent tip speed, $U_t/\sqrt{\theta^*_1}$, ft/sec	602
Equivalent weight flow per unit annulus area, $w\sqrt{\theta^*_1}/\delta_1 A_1$, lb/sec/sq ft	14.94
Equivalent weight flow, $w\sqrt{\theta^*_1}/\delta_1$, lb/sec	36.89
Turbine-tip diameter, in.	34.30
Turbine hub-tip radius ratio	0.784
Equivalent shaft work, $\Delta h/\theta^*_1$, Btu/lb	24.82

Design Procedure

The following assumptions were made in the design:

(1) The absolute stagnation pressure and the stagnation temperature are uniform over the blade height at the entrance to the stator and rotor.

(2) The expansion in the turbine is adiabatic.

(3) The stagnation-pressure ratio across the stator p_2'/p_1' equals 0.98.

(4) The ratio of the effective annulus area to the actual annulus area at the stator and rotor exit equals 0.95. (This assumption together with assumption (3) results in a flow coefficient of 0.93 at the stator exit.)

(5) The design brake internal efficiency equals 0.85. (This results in a stagnation-pressure ratio p_1'/p_3' at the mean radius of 2.44.)

A limiting relative rotor-entrance Mach number of 0.85 was assigned at the rotor hub. In accordance with the method based on simplified radial equilibrium in reference 1, preliminary calculations were therefore made to determine the value of rotor-exit tangential velocity that would yield this desired Mach number. The case based on simplified radial equilibrium was used herein for the purpose of expediency. A value of rotor-exit tangential velocity of -225 feet per second yielded a relative Mach number of 0.86 at the hub. It was known that this Mach number would decrease slightly when the effect of curvature of the streamlines in the radial-axial plane was accounted for. This value of rotor-exit tangential velocity was therefore considered to be satisfactory with regard to the limiting relative rotor-entrance Mach number at the rotor hub. This value of rotor-exit tangential velocity (-225 ft/sec) together with the design requirements, assumptions, and the charts of references 1 and 4 was used to calculate velocity diagrams for the hub, mean, and tip radii at the stator and rotor exits for a fuel-air ratio of 0.018; a fuel having a hydrogen-carbon ratio of 0.167 was used. The design of the stator and rotor blades was based on the velocity diagrams obtained when curvature of the streamlines in the radial-axial plane was accounted for (in accordance with reference 1); however, for comparative purposes, the velocity diagrams based on simplified radial-equilibrium were also calculated. The results for both cases are presented in figure 1. A hub relative rotor-entrance Mach number of 0.84 exists if the curvature of the streamlines in the radial-axial plane is accounted for; also, although large variations of the flow conditions exist between these two cases, the variation in blade angles is small. The data presented in figure 1 yielded values of integrated equivalent weight flow of 37.11 pounds per second and equivalent-weight-flow-averaged shaft work of 24.78 Btu per pound, which closely satisfied the design specifications.

2459

Blade Design

The turbine design was intended for use in a contemporary turbojet engine; therefore, geometric departures from the design of the existing turbine were held to a minimum and were made only when simplicity of cooling the rotor blades would result. Consequently, the parameters of solidity, aspect ratio, axial chord, blade height, and leading- and trailing-edge radii of the existing turbine were maintained in the design of the stator blades. As a means of simplifying the problem of cooling the rotor blades, changes in the existing rotor-blade parameters were adopted. The number of rotor blades was reduced from 96 to 72 blades and the axial chord was changed from 1.68 inches to 2.25 inches. In

this manner, the same rotor-blade solidity (based on axial chord) was maintained. The rotor-blade height of the existing turbine was used; a change in aspect ratio (based on axial chord) from 2.20 to 1.64 resulted. Details of the stator- and rotor-blade profile designs are presented in the following sections.

Stator blades. - The stator-blade exit angles as presented in the velocity diagrams in figure 1 are the flow angles in the free space between the stator exit and rotor entrance and do not account for blockage due to the trailing edge of the stator blade. The stator-blade suction-surface exit angles were determined by accounting for trailing-edge blockage in the following manner: A trailing-edge radius equal to the trailing-edge radius of the existing blade was used and a weight-flow parameter $\frac{\rho_2 V_{x,2}}{\rho_2' a_{cr,2}}$, based on the restricted area was determined. The absolute velocities at the stator exit as presented in the velocity diagrams indicate that supersonic velocities exist in the free space between the stator exit and rotor entrance. It was therefore assumed that sonic velocity exists at the stator-blade throat. With the use of figure 4 of reference 1, the absolute flow angle was calculated for the value of weight-flow parameter based on the restricted area and for the condition of sonic absolute velocity. This angle was assumed to be the stator-blade suction-surface exit angle at the throat of the blade. A straight section on the suction surface was maintained from the throat to the trailing-edge radius and the remainder of the profile was determined by fairing between the leading-edge radius and the throat for the suction surface and by fairing between the leading- and trailing-edge radii for the pressure surface maintaining a smooth variation of flow passage between adjacent blades. This procedure was followed at the hub, mean, and tip radii and the entire blade was constructed by fairing between the sections at these radii. For expediency, no analysis of the flow conditions through the stator-blade passages was made. The mean-section profile is presented in figure 2 together with a comparison of the stator-blade-profile exit angles and the stator-exit flow angles at the hub, mean, and tip radii.

Rotor blades. - Cooling requirements imposed certain limitations on the rotor-blade profile design. The cooling requirements specified were (1) that the internal cooling-air passage area and profile not change along the blade height, and (2) that the minimum leading- and trailing-edge radii of the cooling-air passage be sufficiently large to provide adequate cooling at the blade extremities. The use of a profile with uniform camber and no twist along the blade height satisfied condition (1). Condition (2) dictated the use of large leading- and trailing-edge radii in the blade profile and consequently resulted in a thick profile in order to maintain a smooth profile from the leading to the trailing edge. With the data presented in the velocity diagrams of figure 1, a rotor-blade profile was designed at the mean radius for zero rotor-entrance

incidence angle. The rotor-blade exit angle was adjusted to account for blockage due to the trailing edge in a manner similar to that used in the stator-blade design except that the rotor-exit tangential velocity was assumed to be constant from the station in the free space at which the velocity diagrams were calculated to the exit of the rotor-blade passage.

The blade profile was constructed as follows: The blade camber line was specified as a third-degree polynomial with slopes at the entrance and exit equal to the tangents of the relative rotor entrance angle and adjusted relative exit angle, respectively. An NACA 65-015 airfoil was then constructed around this camber line and the profile was modified until the cooling requirements were satisfied. The final mean-radius profile is shown in figure 3. A ratio of the trailing-edge thickness to pitch of 0.094 exists at the mean radius and the adjusted, relative rotor-blade exit angle equals 137.0° as compared with the exit flow angle of 142.2°. In accordance with reference 2 this value of the ratio of the trailing-edge thickness to pitch indicates that additional blade losses should be expected. In order to determine the average flow conditions along the rotor-blade surfaces, the flow conditions within the blade passage at the mean radius were analyzed in accordance with the method presented in reference 5. The results of this analysis for the channel portion of the blade passage are presented in figure 4 where the suction- and pressure-surface relative critical-velocity ratios are plotted against surface distance. This figure shows that a maximum relative critical velocity ratio of 1.05 occurs on the suction surface at a distance 0.81 inch along the surface (24 percent of the surface length). The profile shown in figure 3 was used at all radii; an untapered, nontwisted rotor blade resulted.

EQUIPMENT AND INSTRUMENTATION

The turbine used in this investigation was a 0.437 scale model of the design that fitted an existing turbine rig. The scale-model stator-blade ring assembly and rotor-blade wheel assembly are shown in figures 5 and 6, respectively. The arrangement of the experimental equipment used is diagrammatically shown in figure 7. Ambient air was drawn from the test cell through an electrostatic precipitator to remove dust particles. The air was then heated by passage through a steam heater to avoid water condensation in the turbine. Constant turbine-entrance temperature was maintained by an automatic control which regulated the amount of air bypassing the heater. After passing through the turbine, the air was exhausted by the laboratory low-pressure exhaust system. An automatically controlled butterfly valve downstream of the surge tank in the low-pressure exhaust line maintained the desired pressure ratio across the turbine.

The power output was absorbed by a water brake that was cradle mounted for torque measurements which were made with a commercial springless dynamometer scale. The turbine speed was indicated by a calibrated electric tachometer. Air flow was measured by means of a standard flat-plate orifice located between the precipitator and the steam heater and installed in conformance with A.S.M.E. specifications.

A cross-sectional view of the turbine showing the location of the instrumentation is presented in figure 8. Entrance stagnation pressures and temperatures were measured by eight stagnation-type probes (four for stagnation pressure and four for stagnation temperature) located at the mean radius at equal circumferential stations 0.73 inch upstream of the stator. The rotor-exit static pressure was measured with 14 static wall taps located 0.66 inch downstream of the rotor, six on the outer wall and eight on the inner wall. The rotor-exit total temperature was measured with four stagnation-type temperature probes located at the mean radius at the downstream end of the exhaust-guide annulus. Although radial variation of the temperature may have prevented the thermocouples from indicating an accurate average temperature, the effect on turbine performance is small because this temperature was used only to compute the available rotor-exit stagnation pressure, in which case an error of 5° R would change the computed efficiency less than 0.003. This method of obtaining exit stagnation pressure is described in the section entitled "PROCEDURE AND PERFORMANCE CALCULATIONS."

In addition to the instrumentation described in the foregoing paragraphs, the turbine rig was equipped with a survey mechanism which enabled detailed surveys to be made of the flow conditions at the stator and rotor exits. This mechanism consisted of a complete circumferential ring with five mounting pads between the stator and rotor and five at the rotor exit at different circumferential stations. On these pads probe actuators were mounted which permitted the probes to be moved to any radial position within the annulus and to be rotated about their axes to any angle in the air stream. The entire survey ring could also be rotated 30° circumferentially by means of a worm and gear drive arrangement.

The instruments were read with the following precision:

Absolute pressure, in. of tetrabromoethane	±0.05
Orifice pressure drop, in. of water	±0.05
Temperature, $^{\circ}$R	±1
Torque load, lb	±0.2
Rotative speed, rpm	±10

For a stagnation-pressure ratio of 2.00 or greater, the probable error in reproducing the turbine efficiency was 0.005.

PROCEDURE AND PERFORMANCE CALCULATIONS

Over-all Performance

Data were taken at nominal values of stagnation-pressure ratios from 1.5 to 3.0. At each of the pressure ratios, the turbine was operated at constant equivalent tip speeds ranging from 350 to 700 feet per second, which correspond to turbine tip speeds of 688 to 1376 feet per second for a turbine-entrance temperature of 2065° R. For all runs, the entrance stagnation temperature was maintained between 683° and 687° R; the stator-entrance stagnation pressure varied between 24 and 26 inches of mercury absolute, depending on the air flow and the ambient-air pressure.

The brake internal efficiency, which is based on expansion between the entrance and exit stagnation pressures, was used to express the performance of the turbine; this efficiency is defined as

$$\eta_t = \frac{\Delta h}{(h_1' - h_3')_s}$$

where Δh is determined from turbine-shaft work. This turbine-shaft work includes the losses of the antifriction bearings which were used in the rig. This manner of measuring the work output is indicative of the power available to the compressor of a jet engine. The ideal drop in enthalpy $(h_1' - h_3')_s$ was computed from the chart of air properties in reference 3 by using the entrance stagnation pressure and temperature and the exit stagnation pressure. The available exit stagnation pressure was computed on the assumptions that one-dimensional flow exists and occupies the full annulus area and that the tangential velocity equals zero at this station by using the following formula in which all quantities are known except p_3':

$$\frac{w\sqrt{T_3'}}{p_3 A_3} = \frac{p_3'}{p_3}\sqrt{\left(\frac{p_3}{p_3'}\right)^{\frac{2}{\gamma}} - \left(\frac{p_3}{p_3'}\right)^{\frac{\gamma+1}{\gamma}}}\left[\left(\frac{2\gamma}{\gamma-1}\right)\left(\frac{g}{R}\right)\right]^{\frac{1}{2}}$$

Because of the assumption of zero exit tangential velocity, this method of computing the available exit stagnation pressure gives a conservative value. If the energy in this tangential velocity is neglected, the design stagnation-pressure ratio changes from 2.44, as previously noted, to 2.45. This pressure ratio and the design shaft work results in an assumed brake internal efficiency of 0.84. The weight flow of air was determined from the orifice measurements and the data of reference 6.

All turbine-performance data were reduced to NACA standard sea-level conditions at the stator entrance. The performance was expressed in terms of the following variables: brake internal efficiency η_t, stagnation-pressure ratio p_1'/p_3', equivalent shaft work $\Delta h/\theta^*_1$, ratio of equivalent tip speed to equivalent weight flow $U_t\delta_1/w\theta^*_1$, and equivalent tip speed $U_t/\sqrt{\theta^*_1}$.

Because the turbine was designed for an entrance temperature of 2065° R and the turbine was tested as a scale model at an entrance temperature of 685° R, some of the design parameters presented in the section TURBINE DESIGN are not directly applicable to the results of the turbine investigation. In order to obtain a comparison of these parameters at different temperature levels, an analysis is presented in appendix B that provides for a comparison of the design parameters at different temperature levels. In this analysis, it was assumed that the parameters of equivalent shaft work and equivalent tip speed are a function of only the ratio of the critical velocity at the turbine-entrance temperature to the critical velocity at the NACA standard sea-level temperature. In the analysis, the parameters of stagnation-pressure ratio and equivalent weight flow are shown to be a function of the ratio of the specific heats. Application of this analysis results in the following scale-model-turbine design parameters for a temperature of 685° R; that is, a specific-heats ratio of 1.40:

Equivalent tip speed, $U_t/\sqrt{\theta^*_1}$, ft/sec	602
Equivalent weight flow per unit annulus area, $w\sqrt{\theta^*_1}/\delta_1 A$, lb/sec/sq ft	15.58
Equivalent weight flow, $W\sqrt{\theta^*_1}/\delta^*_1$, lb/sec	7.37
Equivalent shaft work, $\Delta h/\theta^*_1$, Btu/lb	24.82
Stagnation-pressure ratio, p_1'/p_3'	2.60
Brake internal efficiency, η_t	0.84

Flow Survey

In order to study the variations of the actual flow conditions from the assumed flow conditions, detailed radial and circumferential measurements of the flow conditions at stator and rotor exits were made simultaneously at approximately the design stagnation-pressure ratio and equivalent tip speed. At the stator exit, the flow angle and the stagnation pressure were measured; the flow angle was measured with a static

wedge probe and the stagnation pressure with a 0.030-inch inside diameter hook-type probe. The flow angle, stagnation pressure, and stagnation temperature were measured at the rotor exit. The flow angle and stagnation pressure were measured with a hook-type three-claw probe, the angle being measured by the outer tubes of the claw and the stagnation pressure by the center tube. An unshielded spike-type thermocouple was used to measure the stagnation temperature at the rotor exit.

RESULTS AND DISCUSSION

Over-all Performance

The over-all performance of the scale-model turbine is presented in the form of a composite plot where the parameters of brake internal efficiency, equivalent tip speed, and stagnation-pressure ratio are plotted against the equivalent shaft work as the ordinate and the ratio of the equivalent tip speed to the equivalent weight flow as the abscissa (fig. 9). At the design equivalent shaft work, 24.82 Btu per pound, and the design equivalent tip speed, 602 feet per second, an efficiency of 0.82 was obtained. At this point a stagnation-pressure ratio of 2.65 exists. This value differs from the design pressure ratio of 2.60 because of the 0.02 difference between the assumed turbine efficiency and that obtained from the investigation.

The lines of constant equivalent tip speed are vertical for all stagnation-pressure ratios above 1.8. This condition indicates that the turbine is choked. The value of choking weight flow, 7.57 pounds per second, which was observed at all speeds indicated that the stator was choked. This value is 2.7 percent greater than that of the design equivalent weight flow. A design flow coefficient of 0.93 was assumed and the stator blade was designed to choke at the throat. A fabrication error of 0.001 inch in the throat width of the model turbine results in a 0.5 percent change in weight flow. Inasmuch as the fabrication tolerances in the throat width were ±0.004 inch, the difference between the design and equivalent weight flow is attributed to fabrication errors and to a variation in the values of the design flow coefficient and the actual flow coefficient.

As can be seen in figure 9, the maximum brake internal efficiencies of the order of 0.845 occurred at regions of stagnation-pressure ratios and equivalent tip speeds higher than design. This condition is believed to exist when the value of the ratio of the mean blade speed to the jet velocity is approximately 0.5, where the jet velocity is defined as:

$$V_j = \sqrt{2gJ\,(h_1' - h_3')_s}$$

A plot of the brake internal efficiency against the ratio of the mean blade speed to the jet velocity for several stagnation-pressure ratios is presented in figure 10. For stagnation-pressure ratios of 1.5, 1.9, and 2.3, peak brake internal efficiency occurs at values of the mean-blade-speed to jet-velocity ratio ranging from 0.50 to 0.52. Peak brake internal efficiencies at the stagnation-pressure ratios of 2.65 and 3.0 were not obtained because the range of speed operation in this investigation did not include the high speeds required to cover this range of mean-blade-speed to jet-velocity ratios for the higher stagnation-pressure ratios.

Flow Survey

Surveys of the flow conditions at the stator and rotor exits were made for a stagnation-pressure ratio of 2.40 and equivalent tip speed of 590 feet per second. The actual brake internal efficiency at this survey point was lower than the assumed value. Inasmuch as the surveys were made at a stagnation-pressure ratio and at a brake internal efficiency lower than design, underturning of the flow at the rotor exit was expected.

Stator exit. - The results of the stator-exit surveys are presented in figures 11 and 12. Figure 11 presents a plot of the measured stagnation-pressure ratio across the stator and the stator-blade-exit flow angle, both parameters measured at the hub, mean, and tip radii, against circumferential position covering two blade passages. It can be seen that large regions of stagnation-pressure loss exist across a blade pitch even at the mean radius. This condition was most severe at the hub radius. The regions of stagnation-pressure loss are larger than could be reasonably attributed to the thickness of the trailing edge of the stator blade. These large regions of stagnation-pressure loss together with the dirt patterns on the stator shrouds indicate that flow separation occurred on the suction surface of the stator blade. Inasmuch as the stator blades were designed to choke at the throat and that the flow separation appeared to occur after the throat, it is probable that these regions of stagnation-pressure loss had little effect on the weight flow through the turbine. A maximum variation of approximately 4° of the stator-blade-exit flow angle was measured across a blade passage at the three radial positions investigated. Some of this variation is due to difficulty in measurement of the angles in the circumferential and radial pressure gradient that existed.

A plot of stagnation-pressure ratio across the stator and the stator-blade-exit flow angle against the radius is presented in figure 12. This survey was made along a path where the stagnation-pressure loss was a minimum as determined by circumferential surveys at several radii. Shroud

boundary layers at the hub and the tip of approximately 0.15 inch existed, as indicated by the gradient of stagnation-pressure ratio shown in figure 12. Outside of these regions a stagnation-pressure loss of approximately 2.0 percent was observed. The maximum deviation of measured stator-exit flow angle from the design angle was 1° except for the region near the hub and the tip boundary layers.

Rotor exit. The results of the rotor-exit surveys are presented in figures 13 and 14. Figure 13 presents a plot of the measured stagnation-pressure ratio across the turbine and the rotor-blade-exit absolute flow angle at the hub, mean, and tip radii against the circumferential position covering the same circumferential arc as in the stator surveys. The severe stagnation-pressure-loss regions that existed at the stator exit were not observed at this station; thus, mixing of the flow through the rotor was indicated. At the mean radius, however, there was some indication that pressure gradients existed at intervals equal to the stator-blade spacing; this indicated that the stator stagnation-pressure-loss regions are not completely dissipated as the air passes through the rotor. The angle variation along the circumference at the hub and tip radii appear to be more severe than the variation at the stator exit. Inasmuch as this angle was measured with a three-claw probe, which is sensitive to the pressure gradients, some of the angle variations may be attributed to the sensitivity of the instrument.

The flow conditions at the rotor exit across the radius are presented in figure 14. At this station care was again taken to obtain measurements in such a manner as to minimize the effect of the circumferential pressure gradients on the instrument readings. Figure 14 presents the radial variation of the measured stagnation-pressure ratio across the turbine, the rotor-blade-exit absolute angle, and the stagnation-temperature-drop ratio. No apparent regions of large gradients of stagnation pressure at the hub and tip of the rotor exit were measured with the instrument used. The stagnation-pressure ratio near the tip of the blades remains almost constant whereas the temperature drop decreases with radius towards the tip of the blade; this combination results in a drop in the turbine efficiency toward the tip of the blade. The angle variation presented indicates that an underturning of approximately 12° exists over the blade height. Some of this underturning can be explained by the fact that the survey was made at a stagnation-pressure ratio and a brake internal efficiency lower than design.

SUMMARY OF RESULTS

An experimental investigation of a scale model of a nontwisted rotor-blade turbine having rotor blades suitable for air cooling and

the same design requirements as those of the turbine of a contemporary turbojet engine was conducted. The over-all performance and flow surveys at the stator and rotor exits indicated the following results:

1. At the design equivalent shaft work and design equivalent tip speed, a brake internal efficiency of 0.82 was obtained. Maximum brake internal efficiencies of the order of 0.845 occurred at regions of stagnation-pressure ratios and equivalent tip speeds greater than design for the range of conditions investigated.

2. Large regions of stagnation-pressure loss were present at the stator exit, a condition which indicates possible flow separation on the suction surface of the stator blade.

3. A decrease of turbine efficiency toward the tip of the blade was observed in the flow surveys at the rotor exit.

Lewis Flight Propulsion Laboratory
National Advisory Committee for Aeronautics
Cleveland, Ohio

APPENDIX A

SYMBOLS

The following symbols are used in this report:

A	annulus area, sq ft
a_{cr}	critical velocity, $\left(\frac{2\gamma}{\gamma+1} gRT\right)^{\frac{1}{2}}$, ft/sec
g	acceleration due to gravity, ft/sec^2
h	specific enthalpy, Btu/lb
Δh	turbine specific shaft work, Btu/lb
J	mechanical equivalent of heat, ft-lb/Btu
K	constant
M	Mach number
p	absolute pressure, lb/sq ft
R	gas constant, ft-lb/(lb)($^\circ$R)
r	radius, in.
T	absolute temperature, $^\circ$R
U	blade velocity, ft/sec
V	absolute gas velocity, ft/sec
W	relative velocity, ft/sec
w	gas weight flow, lb/sec
α	angle of absolute velocity with tangential direction, deg
β	angle of relative velocity with tangential direction, deg
γ	ratio of specific heats
δ	ratio of inlet-air pressure to NACA standard sea-level pressure, $\frac{p'}{p_0}$

2459

ϵ function of γ

η_t turbine brake internal efficiency based on stagnation condition

θ^* square of ratio of critical velocity to critical velocity at NACA standard sea-level temperature, $\left(\frac{a_{cr}}{a_{cr,0}}\right)^2$

ρ density, lb/cu ft

Subscripts:

0 NACA sea-level standard

1 stator entrance

2 stator exit, rotor entrance

3 rotor exit

C cold condition

cr critical, state at speed of sound

H hot condition

h turbine hub

j ideal jet

m turbine mean

s isentropic

t turbine tip

th stator throat

u tangential

w relative

x axial

Superscript:

' stagnation state

" relative stagnation state

APPENDIX B

ANALYSIS OF VARIATION OF DESIGN EQUIVALENT PARAMETERS WITH TURBINE-ENTRANCE TEMPERATURE

In the analysis of the comparison of the performance of turbines at different temperature levels, it is most desirable to compare the design parameters that result in similar velocity triangles in which the components of the triangle have equal Mach numbers. The Mach number is a function of the static temperature, which is difficult to determine in a performance investigation. For a single-stage turbine with a choked stator, the absolute Mach number is equal to or only slightly greater than the critical velocity ratio. Therefore, the assumption will be made that all the equivalent velocity parameters are based on the critical velocity, which is defined as $a_{cr}' = \sqrt{\frac{2\gamma}{\gamma+1} gRT'}$. In a single-stage turbine with zero rotor-exit tangential velocity, the work output of the turbine may be expressed in terms of velocity components at the stator exit; that is,

$$\Delta h = \frac{U_2 V_{u,2}}{gJ}$$

The equivalent tip speed and the equivalent shaft work may therefore be expressed as a function of the ratio of the critical velocity at the turbine-entrance temperature to the critical velocity at the NACA standard sea-level temperature; that is,

$$\left(\frac{U_t}{\sqrt{\theta^*_1}}\right)_H = \left(\frac{U_t}{\sqrt{\theta^*_1}}\right)_C$$

and

$$\left(\frac{\Delta h}{\theta^*_1}\right)_H = \left(\frac{\Delta h}{\theta^*_1}\right)_C$$

The variation in the stagnation-pressure ratio with the turbine-entrance temperature is determined as follows. The equivalent shaft work may be expressed as

$$\frac{\Delta h}{\theta^*_1} = a_{cr,0}^2 \frac{\eta_t}{2gJ} \frac{\gamma+1}{\gamma-1} \left[1 - \left(\frac{p_3'}{p_1'} \right)^{\frac{\gamma-1}{\gamma}} \right] \tag{1}$$

Because $\left(\frac{\Delta h}{\theta^*_1}\right)_H = \left(\frac{\Delta h}{\theta^*_1}\right)_C$ and if it is assumed that $R_H = R_C$ and $(\eta_t)_H = (\eta_t)_C$, the following equation results when equation (1) is equated for the hot and the cold conditions:

$$\left\{ \frac{\gamma+1}{\gamma-1} \left[1 - \left(\frac{p_3'}{p_1'} \right)^{\frac{\gamma-1}{\gamma}} \right] \right\}_H = \left\{ \frac{\gamma+1}{\gamma-1} \left[1 - \left(\frac{p_3'}{p_1'} \right)^{\frac{\gamma-1}{\gamma}} \right] \right\}_C \tag{2}$$

This expression gives the relation of the stagnation-pressure ratios for hot and cold conditions as a function of ratio of the specific heats.

The variation in equivalent weight flow with the turbine-entrance temperature is determined as follows: The weight for a choked stator may be expressed as

$$w = \rho_{cr} a_{cr}' A_{th} \tag{3}$$

If it is assumed that $T_{cr}' = T_1'$ and that the pressure losses are such that $\frac{p_{cr}'}{p_1'} = K$ and if the following thermodynamic relations are used for critical flow,

$$\frac{p_{cr}}{p_{cr}'} = \left(\frac{2}{\gamma+1} \right)^{\frac{\gamma}{\gamma-1}}$$

and

$$\frac{T_{cr}}{T_{cr}'} = \frac{2}{\gamma+1}$$

equation (3) may be written as

$$w = A_{th} \frac{p_1'}{a_{cr,1}'} gK\gamma \left(\frac{2}{\gamma+1}\right)^{\frac{\gamma}{\gamma-1}} \tag{4}$$

If it is assumed that the throat areas and the pressure loss through the stator are equal for the hot and cold conditions, the following expression results when equation (4) is equated for the hot and cold conditions:

$$\left[\frac{w a_{cr,1}'}{p_1'} \left(\frac{\gamma+1}{2}\right)^{\frac{\gamma}{\gamma-1}} \frac{1}{\gamma}\right]_H = \left[\frac{w a_{cr,1}'}{p_1'} \left(\frac{\gamma+1}{2}\right) \frac{1}{\gamma}\right]_C \tag{5}$$

When both sides of equation (5) are divided by $a_{cr,0}$ and multiplied by p_0, the ratio of the equivalent weight flows for the hot and cold conditions may be written

$$\frac{\left(\frac{w\sqrt{\theta^*_1}}{\delta_1}\right)_H}{\left(\frac{w\sqrt{\theta^*_1}}{\delta_1}\right)_C} = \epsilon \tag{6}$$

where

$$\epsilon = \frac{\left[\left(\frac{\gamma+1}{2}\right)^{\frac{\gamma}{\gamma-1}} \frac{1}{\gamma}\right]_C}{\left[\left(\frac{\gamma+1}{2}\right)^{\frac{\gamma}{\gamma-1}} \frac{1}{\gamma}\right]_H}$$

REFERENCES

1. Slivka, William R., and Silvern, David H.: Analytical Evaluation of Aerodynamic Characteristics of Turbines with Nontwisted Rotor Blades. NACA TN 2365, 1951.

2. Reeman, J., and Simonis, E. A.: The Effect of Trailing Edge Thickness on Blade Loss. Tech. Note No. 116, British R.A.E., March 1943.

3. Silvern, David H., and Slivka, William R.: Experimental Investigation of an 0.8 Hub-Tip Radius-Ratio, Nontwisted-Rotor-Blade Turbine. NACA RM E51G14, 1951.

4. English, Robert E., and Wachtl, William W.: Charts of Thermodynamic Properties of Air and Combustion Products From 300° to 3500° R. NACA TN 2071, 1950.

5. Huppert, M. C., and MacGregor, Charles: Comparison Between Predicted and Observed Performance of Gas-Turbine Stator Blade Designed for Free-Vortex Flow. NACA TN 1810, 1949.

6. Anon.: Fluid Meters, Their Theory and Application. A.S.M.E. Res. Pub., Am. Soc. Mech. Eng. (New York), 4th ed., 1937.

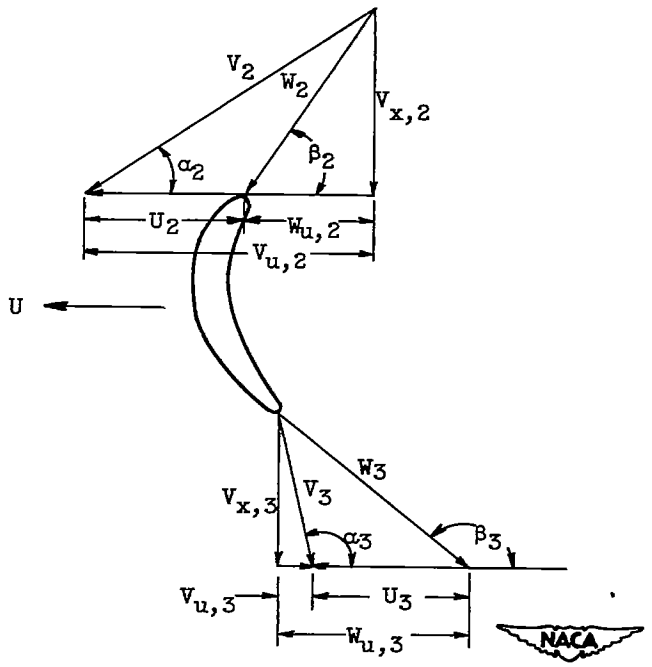

	Simplified radial equilibrium			Streamline curvature accounted for		
	Hub	Mean	Tip	Hub	Mean	Tip
V_2	2442	2188	1974	2422	2188	1988
W_2	1640	1254	900	1619	1254	915
$V_{x,2}$	998	763	548	985	763	557
U_2	927	1055	1183	927	1055	1183
$W_{u,2}$	1302	995	714	1285	995	726
$V_{u,2}$	2229	2050	1897	2212	2050	1909
α_2	24.1°	20.4°	16.1°	24.0°	20.4°	16.3°
β_2	37.5°	37.5°	37.5°	37.5°	37.5°	37.5°
$M_{w,2}$	0.86	0.64	0.45	0.84	0.64	0.46
$M_{v,2}$	1.28	1.11	0.99	1.26	1.11	1.00
V_3	1190	1018	993	1052	1018	1014
W_3	1778	1620	1614	1618	1620	1644
$V_{x,3}$	1090	992	989	991	992	1008
$W_{u,3}$	-1405	-1280	-1276	-1278	-1280	-1300
$V_{u,3}$	- 478	- 225	- 93	- 351	- 225	- 117
α_3	113.7°	102.8°	95.4°	109.5°	102.8°	96.6°
β_3	142.2°	142.2°	142.2°	142.2°	142.2°	142.2°
$M_{w,3}$	0.94	0.84	0.84	0.84	0.84	0.86
$M_{v,3}$	0.63	0.53	0.52	0.55	0.53	0.53
$\beta_3 - \beta_2$	104.7°	104.7°	104.7°	104.7°	104.7°	104.7°

Figure 1. - Comparison of design velocity diagrams based on simplified radial equilibrium and condition where streamline curvature is accounted for.

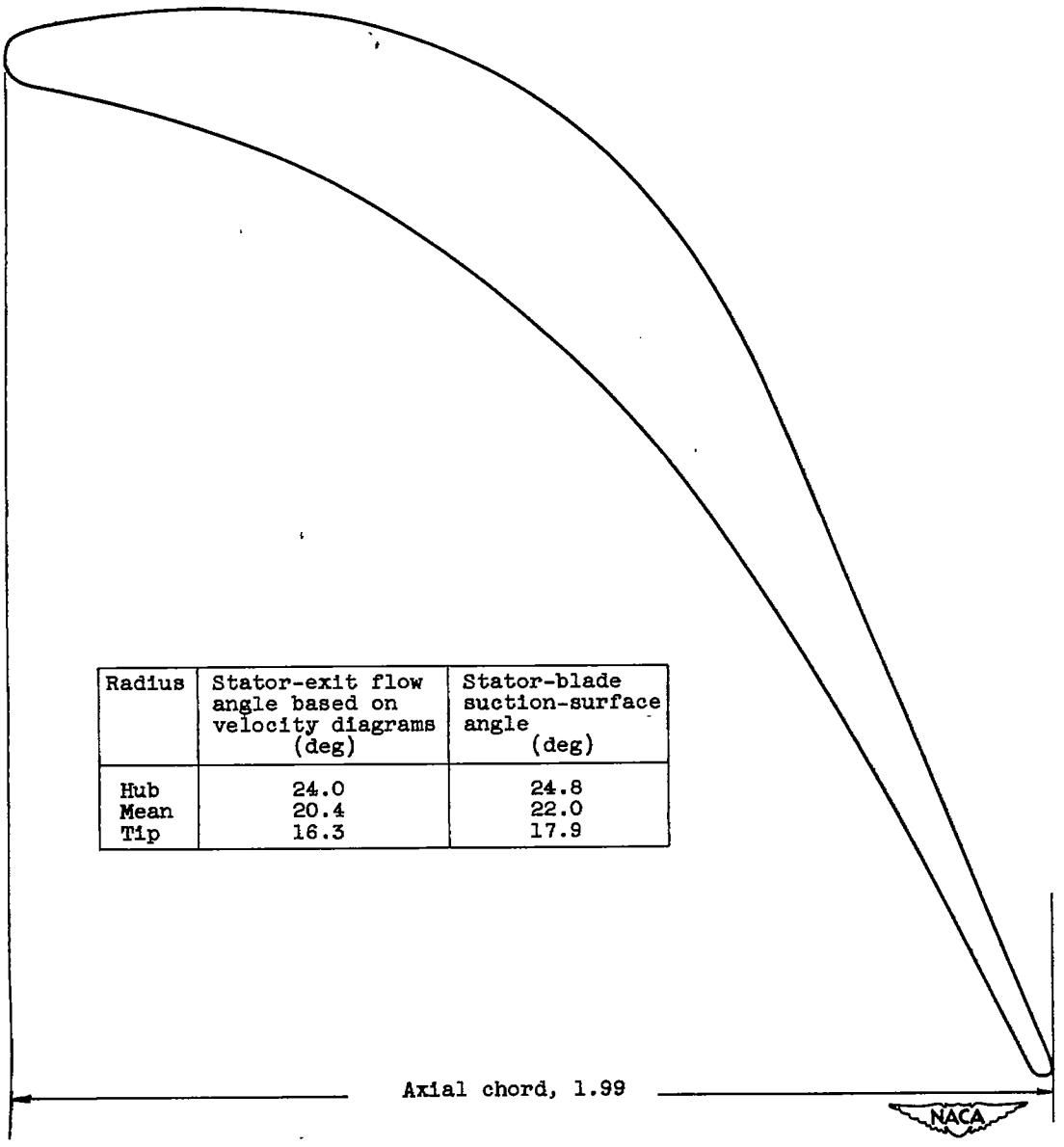

Radius	Stator-exit flow angle based on velocity diagrams (deg)	Stator-blade suction-surface angle (deg)
Hub	24.0	24.8
Mean	20.4	22.0
Tip	16.3	17.9

Figure 2. - Mean-radius stator-blade profile. Pitch, 1.50 inches; solidity based on axial chord, 1.33.

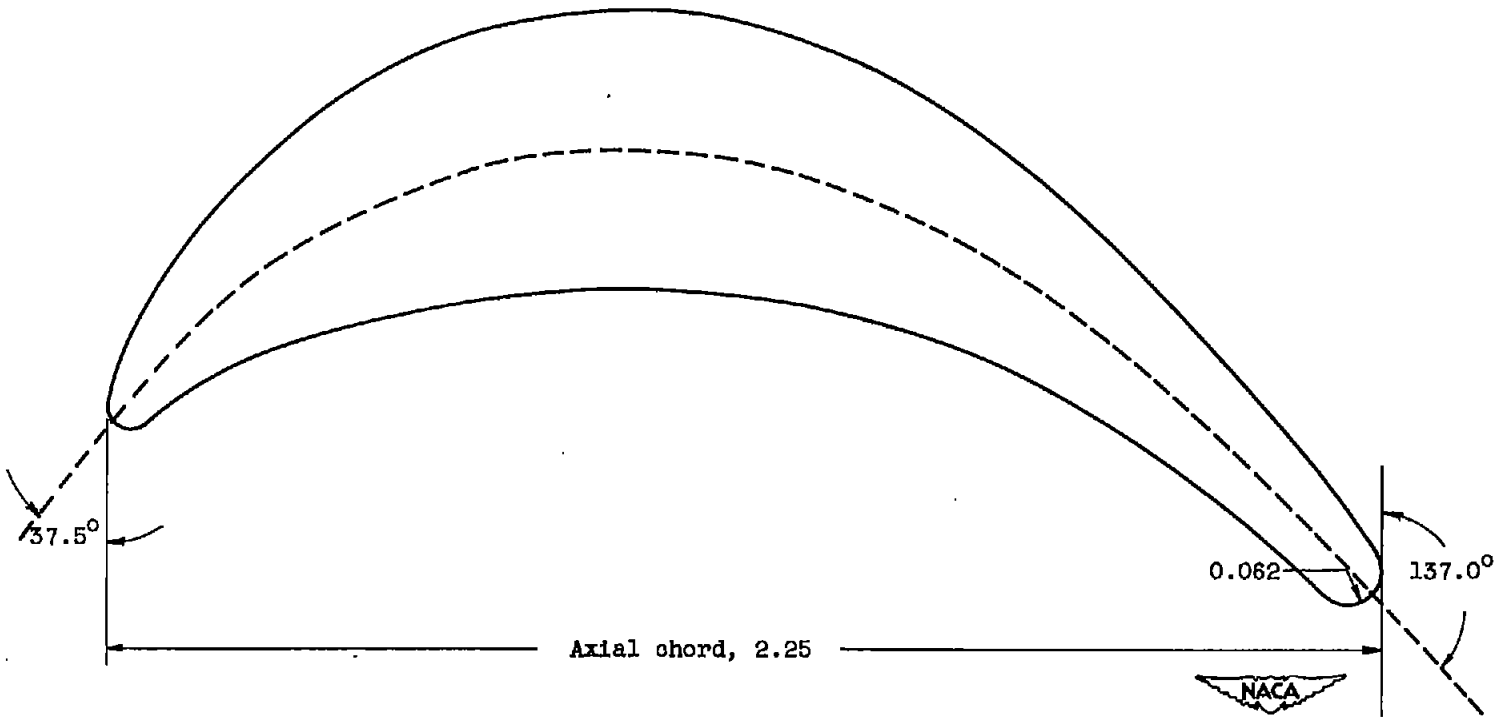

Figure 3. - Mean-radius rotor-blade profile. Pitch, 1.335 inches; solidity based on axial chord, 1.685; ratio of trailing-edge thickness to pitch, 0.094.

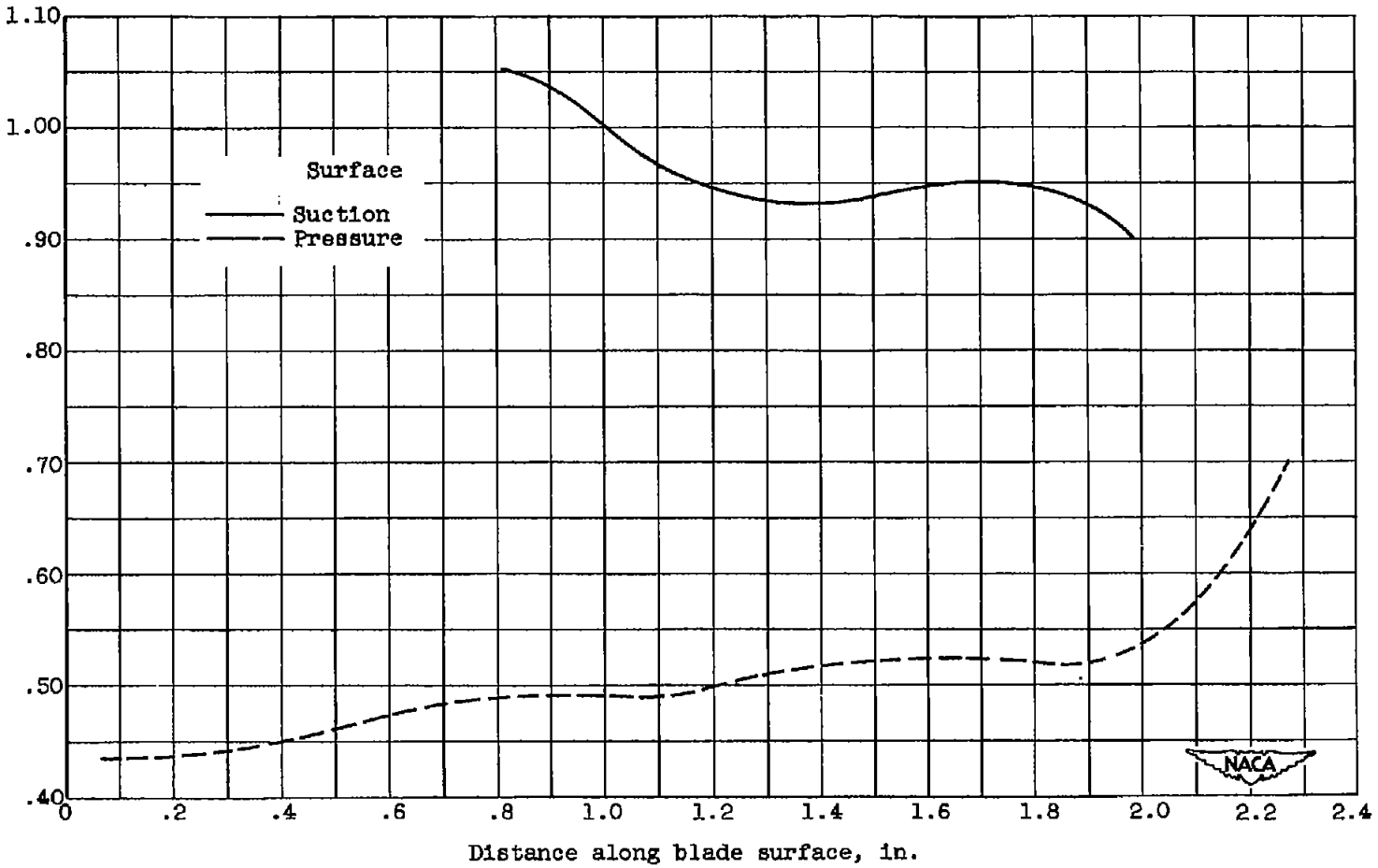

Figure 4. - Rotor-blade surface relative critical-velocity ratio at mean radius.

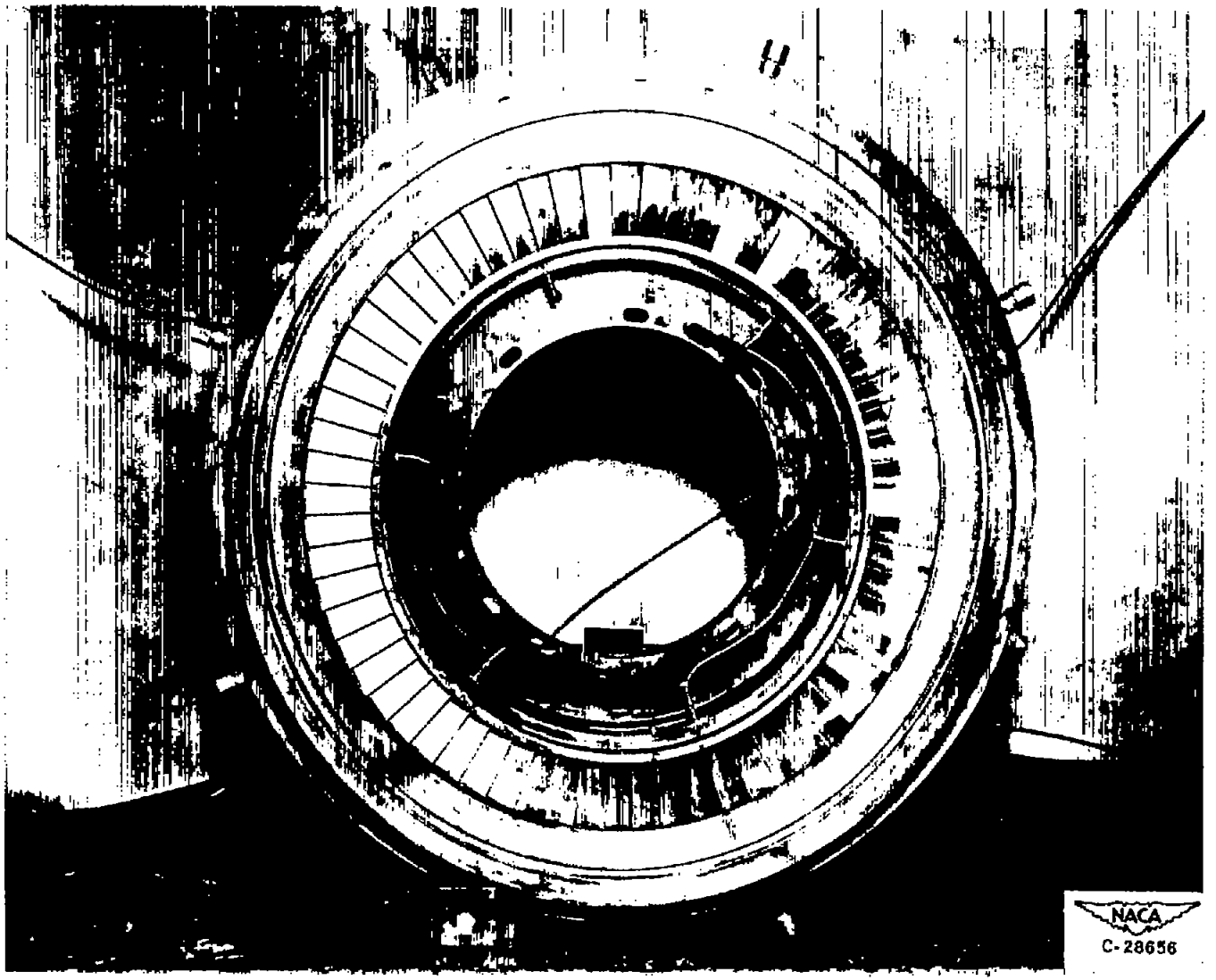

Figure 5. - Scale-model stator-blade ring assembly; downstream view.

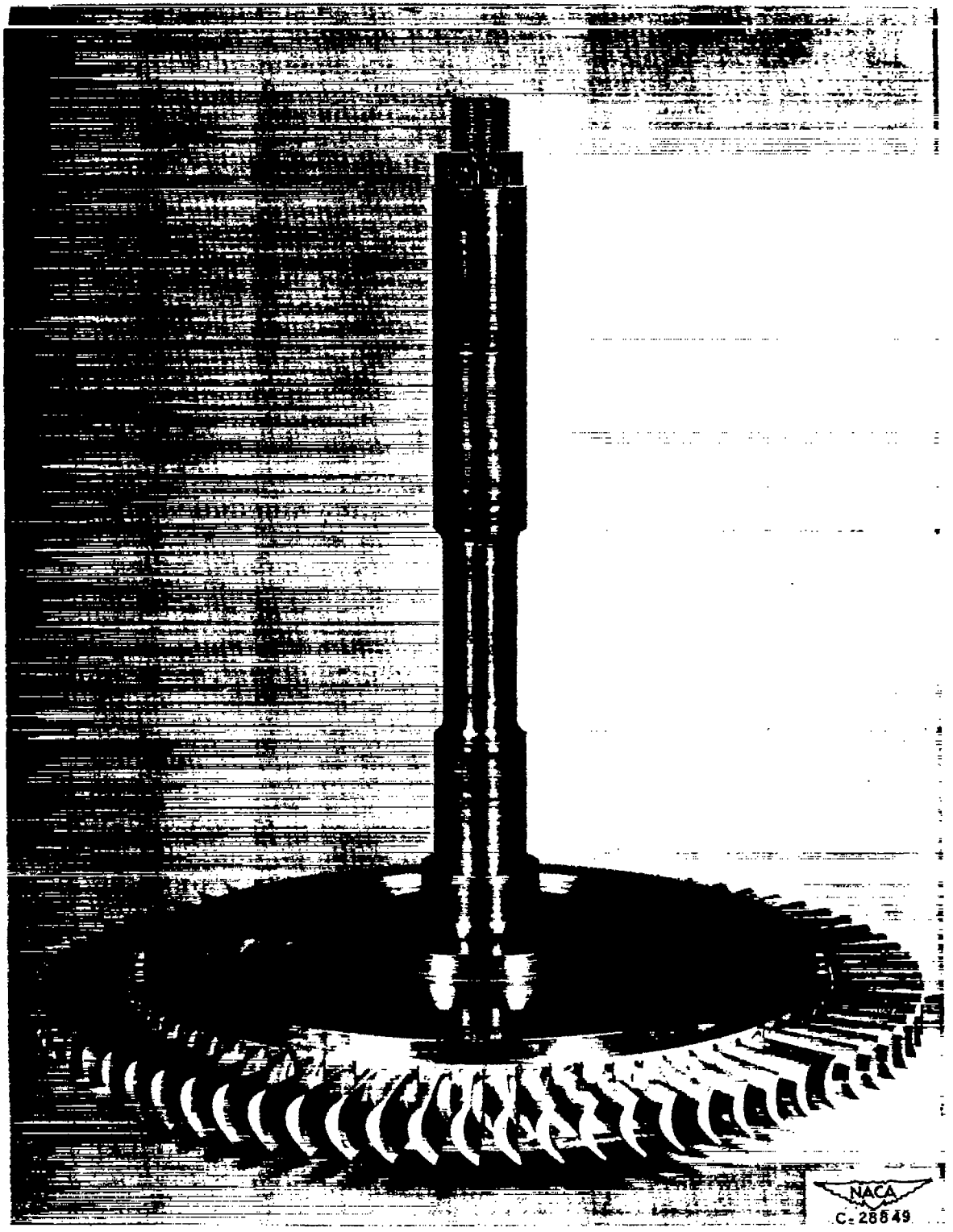

Figure 6. - Scale-model rotor-blade wheel assembly.

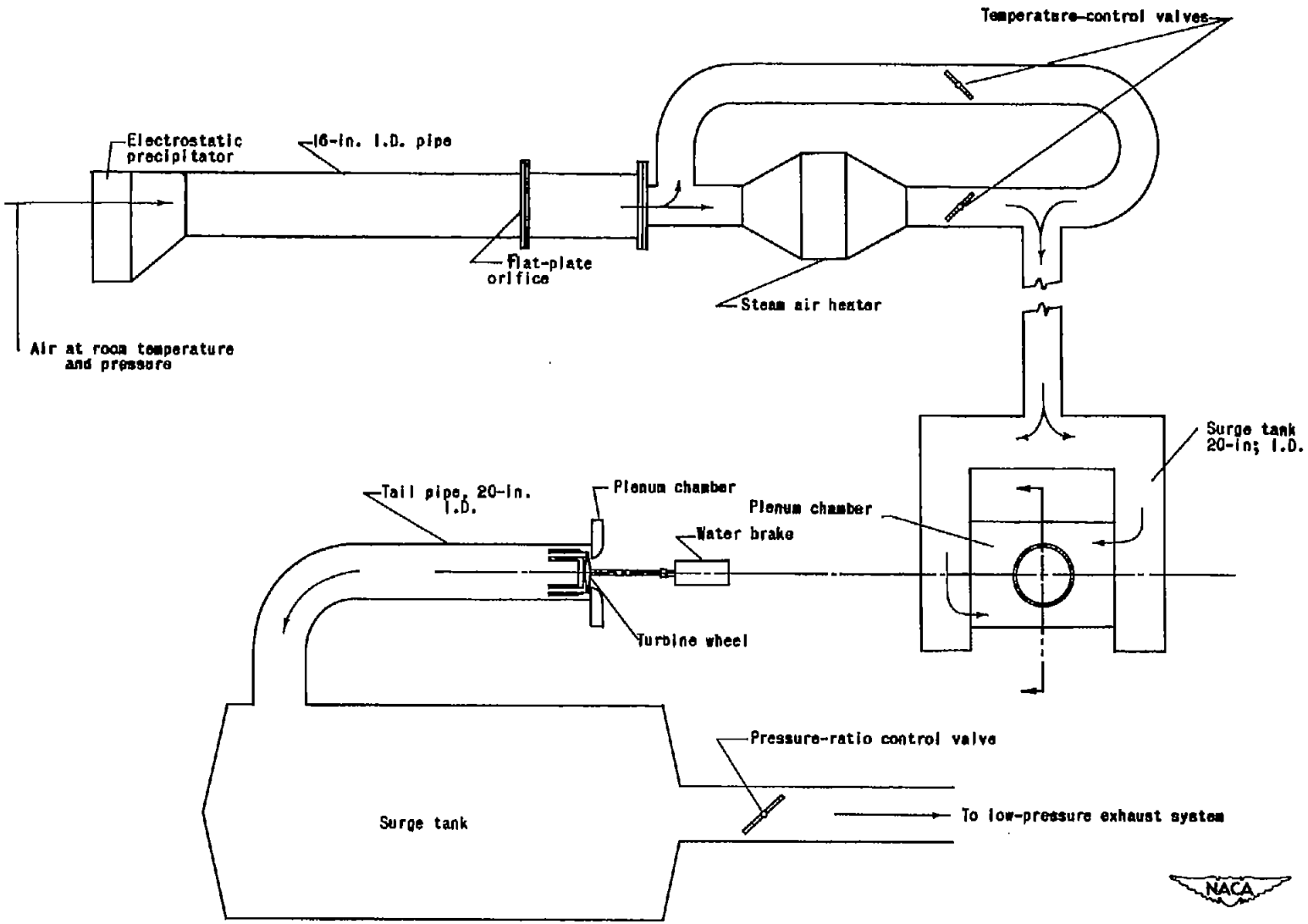

Figure 7. - Diagrammatic sketch of experimental-equipment arrangement showing pressure-ratio control valve, air-flow path, and auxiliary equipment.

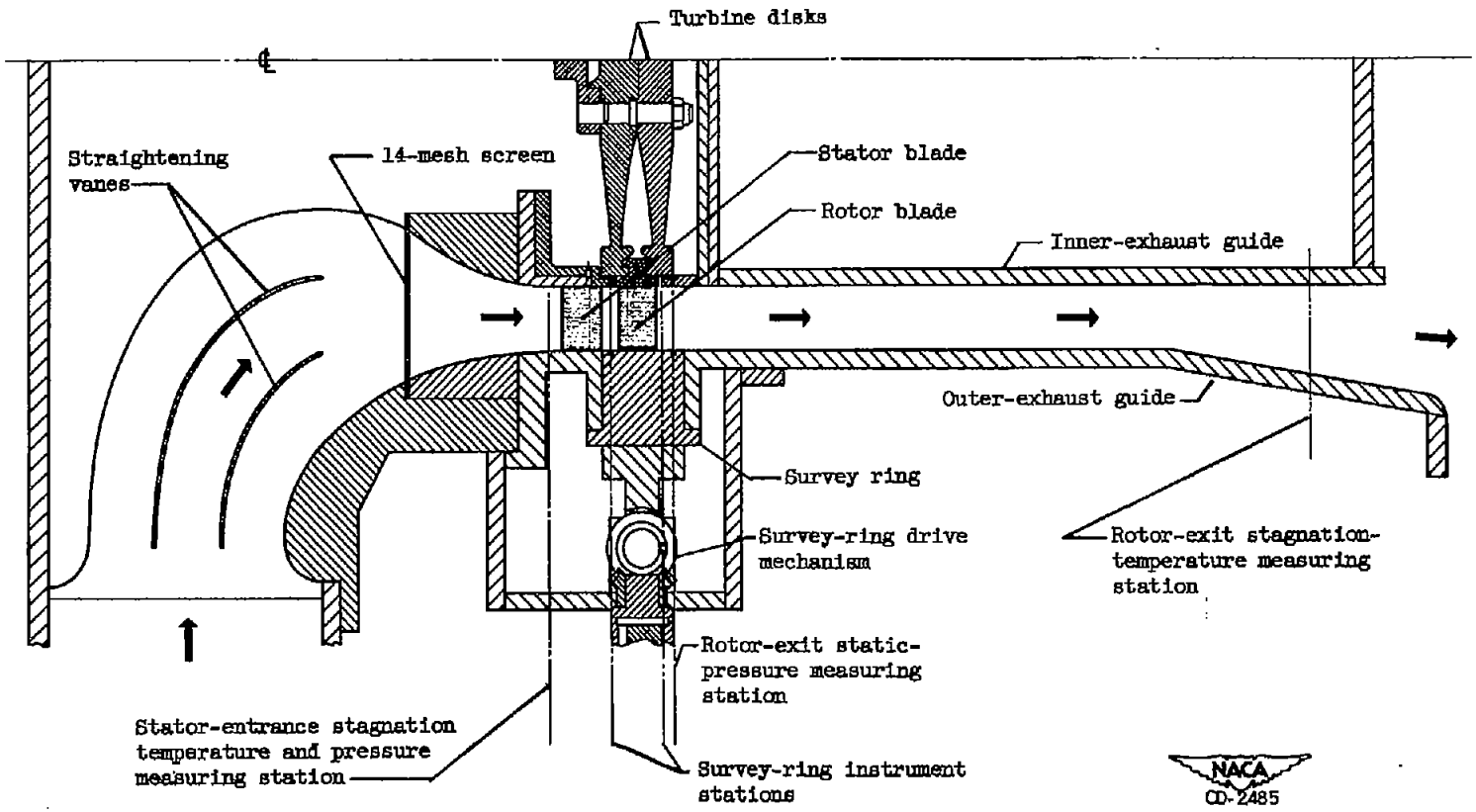

Figure 8. - Cross section of turbine showing instrumentation.

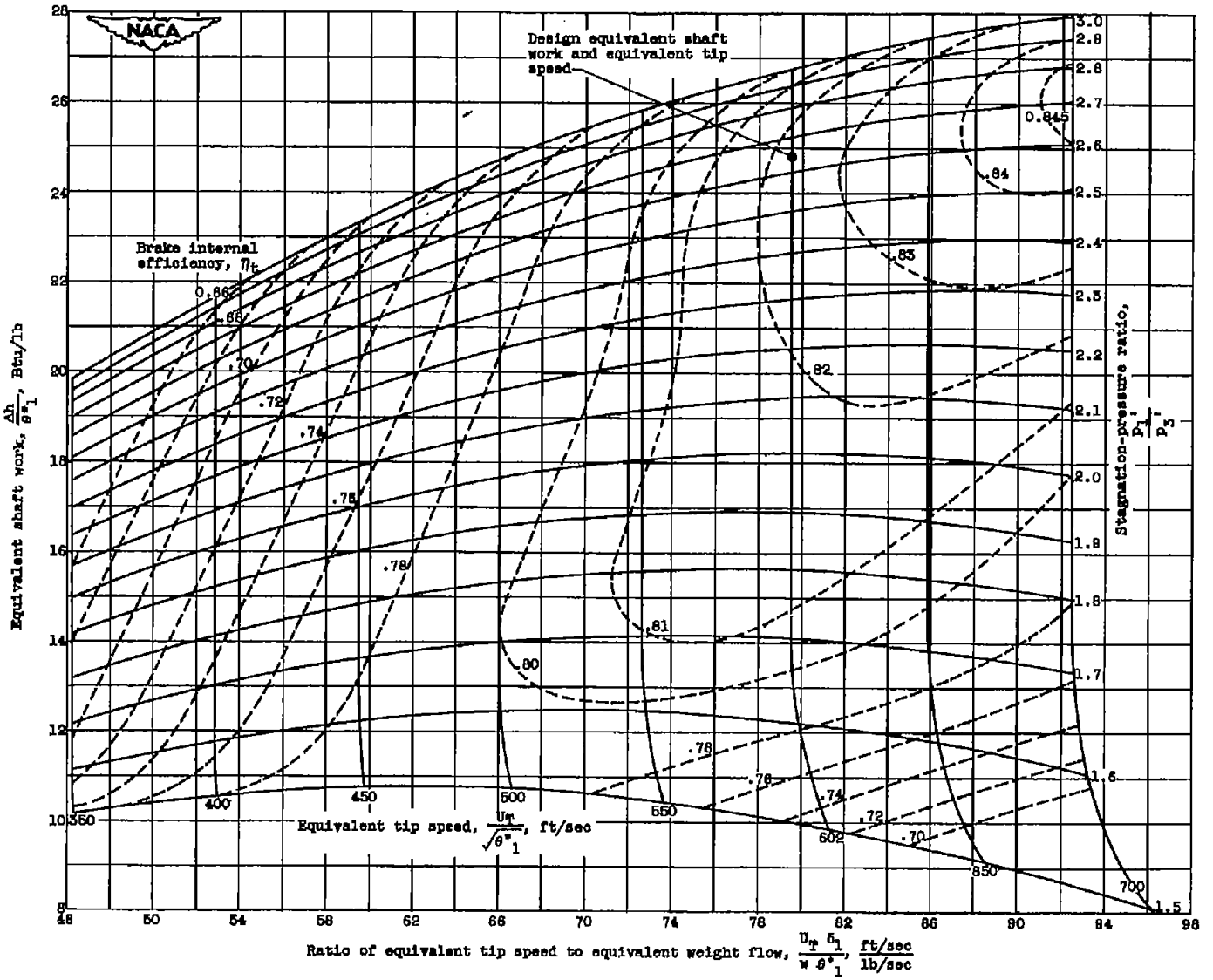

Figure 9. - Over-all performance of scale-model turbine.

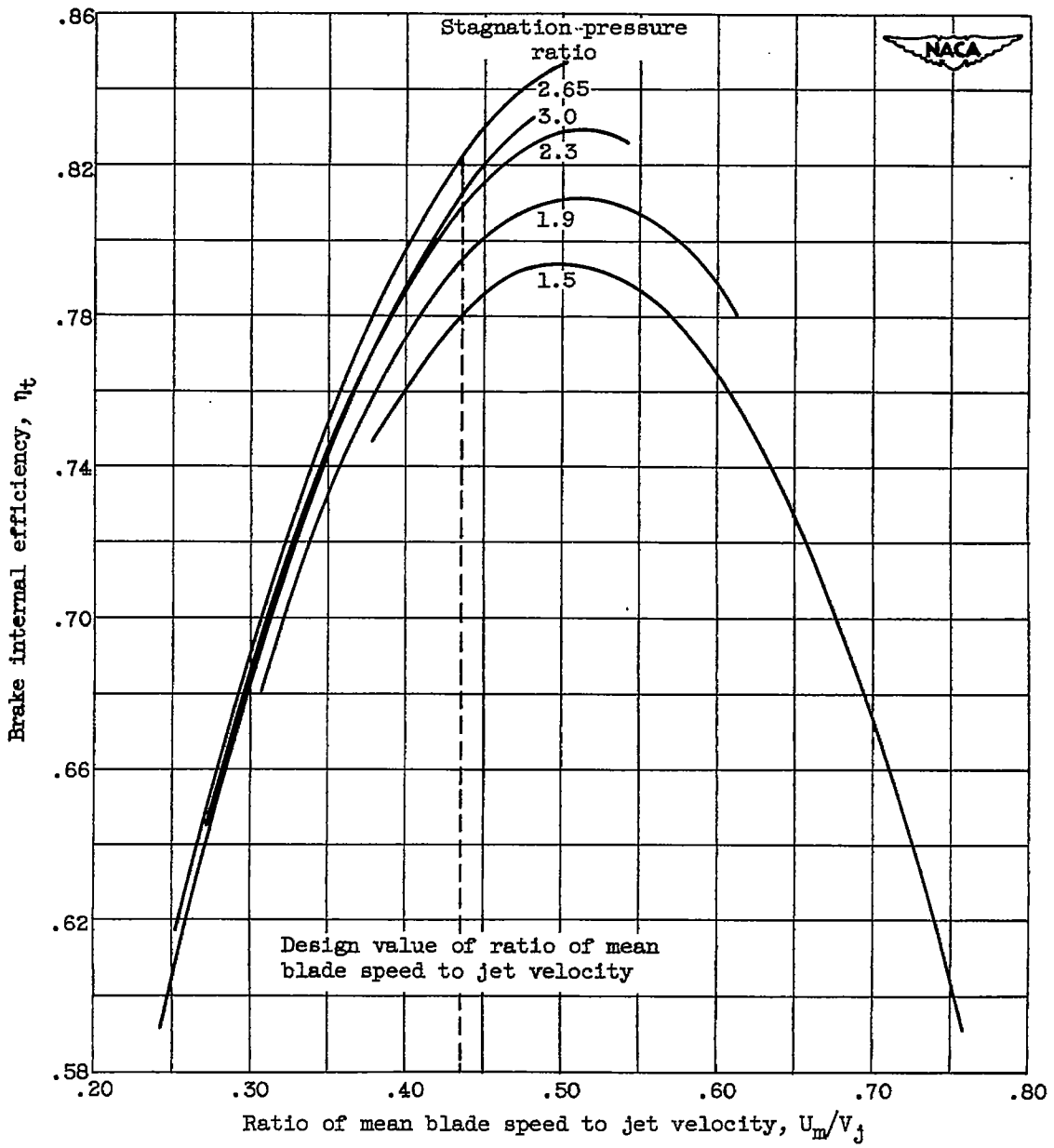

Figure 10. - Variation of brake internal efficiency with ratio of mean blade speed to jet velocity for scale-model turbine. Stagnation-pressure ratio at design equivalent shaft work and equivalent tip speed, 2.65.

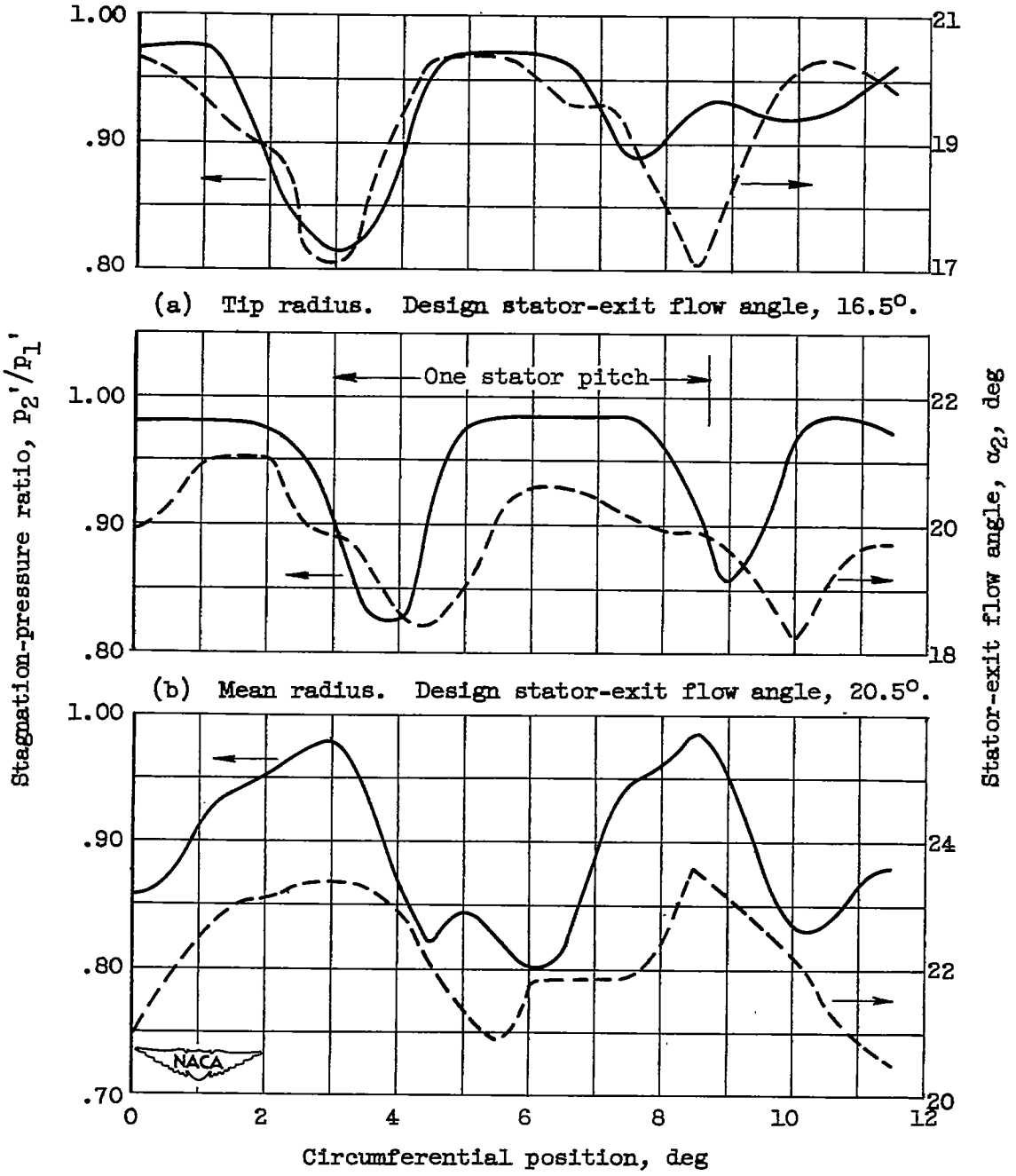

Figure 11. - Circumferential variation in stagnation-pressure ratio and flow angle at stator exit. Turbine stagnation-pressure ratio, p_1'/p_3', 2.40; turbine equivalent tip speed, $U_t/\sqrt{\theta^*_1}$, 590 feet per second.

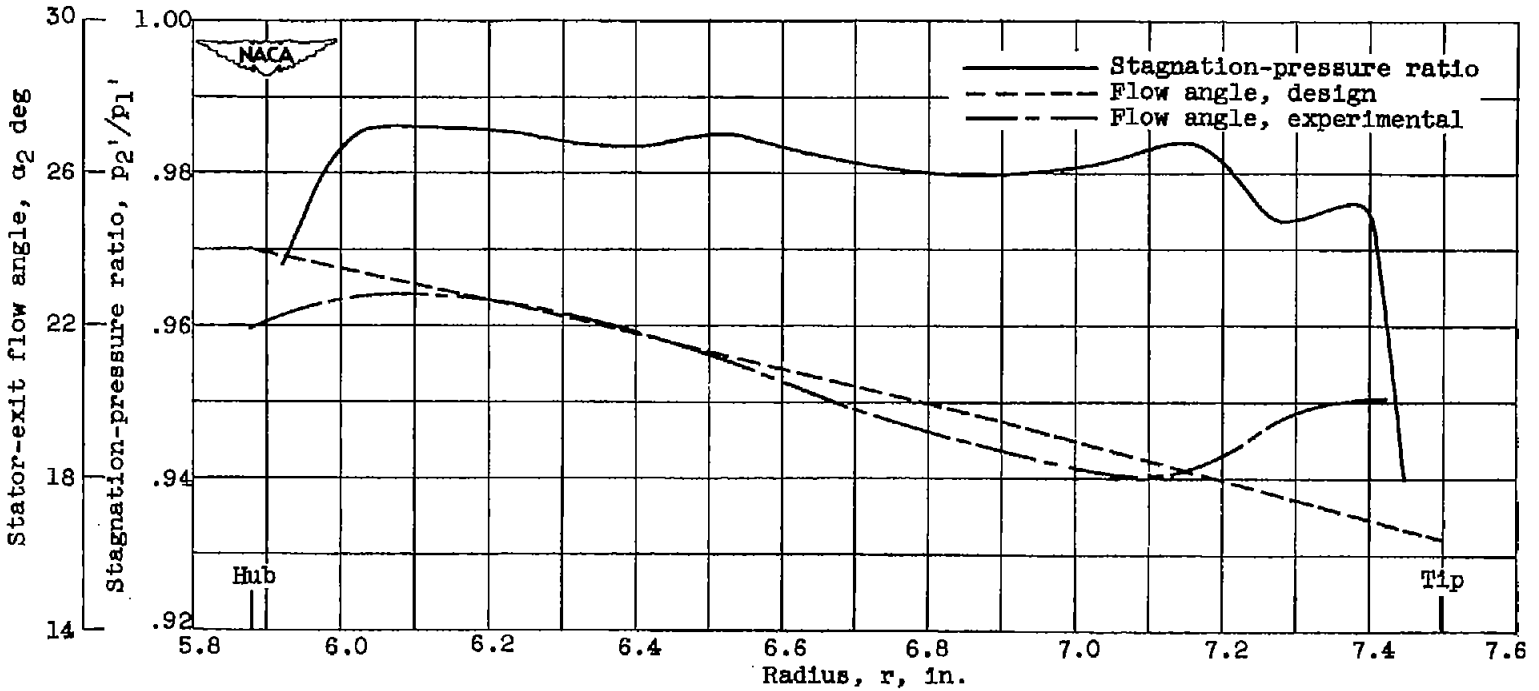

Figure 12. - Radial variation of stagnation-pressure ratio and flow angle at stator exit. Turbine stagnation-pressure ratio, p_1'/p_3', 2.40; turbine equivalent tip speed, $U_t/\sqrt{\theta^*_1}$, 590 feet per second.

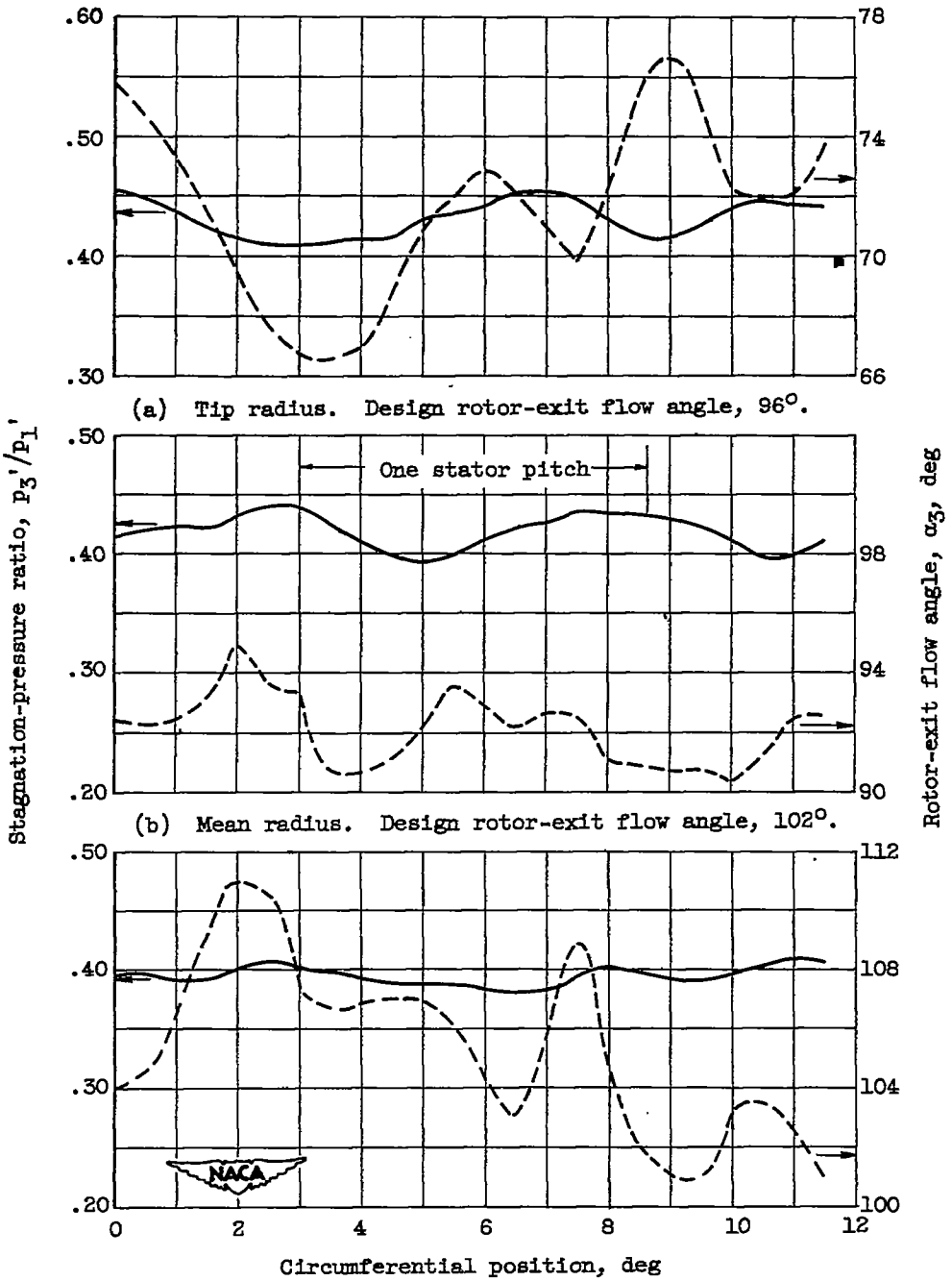

Figure 13. - Circumferential variation in stagnation-pressure ratio and flow angle at rotor exit. Turbine stagnation-pressure ratio, p_1'/p_3', 2.40; turbine equivalent tip speed, $U_t/\sqrt{\theta}_1$, 590 feet per second.

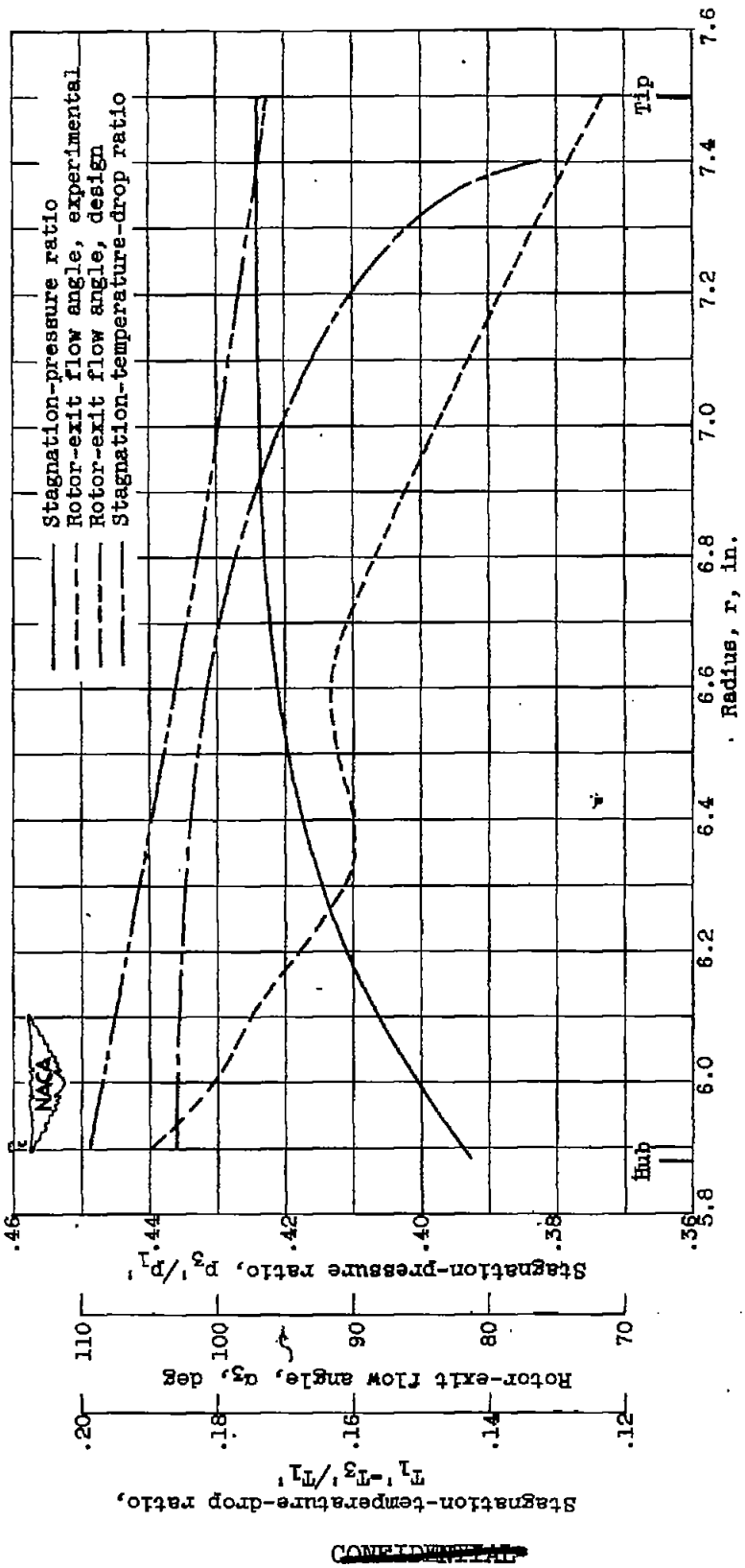

Figure 14. - Radial variation of stagnation-pressure ratio, flow angle, and stagnation-temperature-drop ratio at rotor exit. Turbine stagnation-pressure ratio, p_1'/p_3', 2.40; turbine equivalent tip speed, $U_t/\sqrt{\theta}_1$, 590 feet per second.

NACA-Langley - 3-18-52 - 350